RSC Advances

PAPER

View Article Online
View Journal | View Issue

Cite this: *RSC Adv.*, 2026, **16**, 1121

Aerobic granular sludge as a regenerative system for nutrient removal and metal recovery from landfill leachate

Víctor Guzmán-Fierro, *[ab] Manuel Quiroz,[b] Karla Moscoso,[b] Constanza Arriagada,[b] Carlo Espinoza,[b] Javiera Mansilla,[a] David Contreras, [c] Víctor Campos,[d] Juan José Gallardo-Rodríguez,[e] Gustavo Riveros [b] and Marlene Roeckel[b]

Landfill leachate is a complex and variable wastewater rich in organic matter, ammonium, salts, and metals, with low biodegradability and highly fluctuating composition. Its management still largely relies on energy- and chemical-intensive treatment schemes, making the treatment of raw, undiluted landfill leachate particularly challenging. This study evaluates, at lab scale, the potential of aerobic granular sludge (AGS) for achieving simultaneous pollutant removal and metal recovery in a 2-L column sequencing batch reactor fed with raw, undiluted landfill leachate collected from an active municipal landfill site. The reactor was operated for 198 days without dilution or addition of co-substrates. This operation resulted in stable granulation and high removal efficiencies, 94% for chemical oxygen demand (COD) and 97% for total nitrogen. Cation analysis shows that assimilation reached 600.47 μmol g^{-1} TS, with calcium and magnesium being the predominant cations. Quantitative analyses revealed near-equal contributions from biosorption (53%) and bioaccumulation (47%), with magnesium dominating biosorption and calcium prevailing in bioaccumulation. Then, a partial metal recovery was achieved by desorption with 0.1 M NaCl, without compromising the granule structure, as verified by FTIR and scanning electron microscopy (SEM). However, the desorption process reduced nitrification and denitrification activities by factors of 3.7 and 1.8, respectively, while heterotrophic activity increased by 2.4-fold. Metagenomic analysis revealed microbial shifts following desorption, favouring genera such as *Paracoccus* and *Burkholderia*, which are associated with heterotrophic metabolism. These results demonstrate the potential of AGS as a regenerative biosorbent for treating landfill leachate and recovering metals. This approach supports sustainable and circular strategies for managing landfill leachate and similar complex effluents.

Received 8th August 2025
Accepted 22nd December 2025

DOI: 10.1039/d5ra05817a

rsc.li/rsc-advances

1. Introduction

Landfill leachate is a chemically complex effluent. It contains high concentrations of organic matter, ammonium, heavy metals, and emerging contaminants. Its composition evolves depending on landfill age, waste composition, and operational conditions.[1] In young landfills, acidic conditions enhance metal solubility, while in mature landfills, the methanogenic phases and metal precipitation predominates, reducing their mobility.[2,3] These dynamic fluctuations, along with variable pH, organic loading, and trace metals, create a significant challenge. For these, landfill leachate is particularly difficult to treat biologically. Moreover, its low biodegradability and imbalanced nutrient ratios (C/N) often necessitate multi-stage treatment systems to meet regulatory discharge limits or enable water reuse. With the global expansion of landfilling practices, the generation of high-strength leachate poses increasing environmental risks to soil and water, underscoring the urgent need for efficient, scalable, and sustainable treatment technologies.

Landfill leachate is commonly treated using physico-chemical and biological processes, but these options are often energy- and chemical-intensive and generally do not address metal recovery.[4] In parallel, natural and bio-based sorbents have been evaluated for metal removal from aqueous streams, yet they are usually tested in simplified systems and show limited regeneration.[5] Together, these limitations highlight the need for regenerative biosorbent processes that can treat raw landfill leachate while enabling controlled metal capture.

In this context, AGS has emerged as a robust, compact biotechnology for treating complex, high-strength wastewater,

[a]*Departamento de Ingeniería de Materiales, Facultad de Ingeniería, Universidad de Concepción, Concepción, Chile. E-mail: viguzman@udec.cl*
[b]*Departamento de Ingeniería Química, Facultad de Ingeniería, Universidad de Concepción, Concepción, Chile*
[c]*Departamento de Química Analítica e Inorgánica, Facultad de Ciencias Químicas, Centro de Biotecnología, Universidad de Concepción, Chile*
[d]*Departamento de Microbiología, Facultad de Ciencias Biológicas, Universidad de Concepción, Concepción, Chile*
[e]*Department of Chemical Engineering, CIAIMBITAL Research Centre, University of Almeria, Spain*

including landfill leachate.[6] Among emerging alternatives, AGS stands out for its operational and economic advantages. Comparative studies with other advanced leachate treatment technologies, such as membrane bioreactors and electrochemical oxidation, have further highlighted AGS as a cost-effective and scalable solution, offering high COD removal efficiencies, lower energy demands, and reduced operational costs (Table S1, SI). AGS consists of dense, self-aggregated microbial granules with stratified zones enabling simultaneous aerobic, anoxic, and anaerobic processes within a single reactor.[7] This structural and functional stratification allows for concurrent carbon removal, nitrification, denitrification, and even phosphorus and metal removal, without requiring separate treatment stages. Its excellent settling properties and resistance to hydraulic shear make AGS particularly advantageous under variable loading conditions, while enabling compact reactor configurations with reduced footprint and energy consumption.[8,9] These characteristics make AGS a promising candidate for one-stage biological treatment processes where conventionally activated sludge or membrane-based systems may struggle with biomass retention and operational stability. Its capacity to retain biomass under high loading conditions and its resistance to shock loads make it particularly well-suited for treating chemically diverse leachates. Recent studies have demonstrated that AGS can tolerate elevated levels of ammonium and COD, while maintaining granule integrity and nutrient removal performance.[10,11] Beyond its structural advantages, AGS functionality is primarily driven by its microbial ecology. This ecology comprises ammonia-oxidising bacteria (AOB), nitrite-oxidizing bacteria (NOB), and aerobic heterotrophic bacteria (AHB), each occupying distinct niches within the granule. The oxygen gradients enable spatial separation of metabolic processes, promoting aerobic oxidation near the surface and facilitating denitrification or anaerobic respiration in the core. However, oxygen competition among microbial groups often limits nitrification, as AHB outcompetes AOB and NOB due to their higher oxygen affinity.[12] For these reasons, operational strategies are needed, including oxygen-limiting conditions or controlled nitrite accumulation, to suppress NOB growth and enhance partial nitrification, enabling efficient nitrogen removal. These oxygen-based interactions become even more critical when evaluating the impact of external perturbations, such as desorption steps for metal recovery, on AGS performance and community dynamics.

AGS has shown potential for metal removal and recovery through biosorption and bioaccumulation, mechanisms facilitated by extracellular polymeric substances (EPS) and intracellular accumulation, respectively.[9] While these findings are promising, most investigations to date have been limited to diluted leachates or supplemented systems, which do not reflect the operational challenges of full-strength, undiluted leachate. Despite these promising developments in AGS research, several knowledge gaps remain. The relative contributions of biosorption and bioaccumulation to metal uptake in AGS systems treating undiluted landfill leachate have not been clearly established. Additionally, the impact of cation desorption—a critical step in metal recovery—on the structural stability, metabolic functionality, and microbial community of AGS remains poorly understood. These uncertainties are further compounded by the complexity and variability of landfill leachate, which introduces operational challenges to granule formation and process stability.

In this context, the objective of this study was to evaluate the performance of AGS as a regenerative system for treating raw, undiluted landfill leachate. Specifically, we aimed to: (i) assess simultaneous nutrient removal and metal retention under high-strength leachate conditions without dilution or co-substrate addition; (ii) develop and apply a quantitative approach to distinguish biosorption from bioaccumulation in metal retention, and to test a mild desorption strategy capable of releasing polyvalent cations into a concentrated eluate while preserving granule integrity; and (iii) examine how the desorption step affects granule structure, microbial community composition, and key metabolic activities. In this study, "metal recovery" is therefore understood as the combination of selective metal capture by AGS and the subsequent release of these metals into a reusable liquid stream, while maintaining the structural and functional suitability of the biosorbent for further sorption–desorption cycles. By addressing these objectives, the study provides the foundation for scalable deployment of AGS technology for combined contaminant removal and resource recovery within a circular bioengineering framework.

2. Experimental

2.1. Analytical methods

Parameters such as pH, COD and nitrogen species (nitrite, nitrate, and total ammonia nitrogen (TAN)) were measured by standard methods.[13] Nitrite, nitrate, and TAN were measured spectrophotometrically using a flow injection analyzer (FIAlab, 2500/2700, 1.0607, USA), with a USB400-VIS-NIR detector.[14] Soluble solids (SS), volatile suspended solids (VSS), and total solids (TS) were measured according to Standard Methods (APHA, 1992). The gas produced by the samples from specific anammox (SAA) and specific denitrification activity (SDA) was analyzed using a gas chromatograph (HP 5890 Series II, Hewlett Packard, Avondale, PA, USA).[15] All chemicals used in this study were of analytical grade and were purchased from commercial suppliers (Sigma-Aldrich or Merck), unless otherwise stated.

2.2. Granule characterization

The AGS was characterized for its metabolic, physical, chemical, and microbial properties. These analyses were performed on samples collected before and after the desorption treatment (NaCl 0.1 M).

2.2.1. Metabolic characterization. Metabolic activities of AGS were determined under both aerobic and anaerobic conditions. The specific activities assessed included: specific heterotrophic activity (SHA), specific ammonium-oxidizing activity (SAOA), specific nitrite-oxidizing activity (SNOA), specific anammox activity (SAA), and specific denitrification activity (SDA). SHA, SAOA, and SNOA were evaluated through respirometric batch assays, following procedures previously

described.[16,17] AGS samples were washed three times with phosphate buffer (KH_2PO_4 0.14 g L^{-1} and $K_2HPO_4 \cdot 3H_2O$ 0.9824 g L^{-1}) and transferred into sealed 270 mL glass jars equipped with an optical oxygen sensor (WQ-FDO 925, Global Water Instrumentation, Inc., USA). Approximately 5 mL (1.5 g VSS L^{-1}) of washed granules were added to each jar. The system was maintained at 30 °C and continuously agitated with a magnetic stirrer. Each reactor was aerated for 10 minutes to ensure full oxygen saturation, after which the vessels were sealed to measure endogenous oxygen uptake over 10 minutes. Afterward, substrates were added, and oxygen consumption was monitored for an additional 10 minutes. The substrate concentrations used were: 200 mg C L^{-1} (as sodium acetate) for SHA, 84.8 mg N–NH_4^+ L^{-1} for SAOA, and 148 mg N–NO_2^- L^{-1} for SNOA. Volatile suspended solids (VSS) were quantified after each test, and results were expressed as grams of oxygen or nitrogen consumed per gram of VSS per day (g O_2 or N g^{-1} VSS d^{-1}). SAA and SDA were measured in 150 mL sealed glass vials with OxiTop® Control AN6 sensors (WTW, Weilheim, Germany), following the protocol adapted from Varas *et al.*[18] Each vial contained 40 mL of AGS suspension (1.5 g VSS L^{-1}) in phosphate buffer adjusted to pH 8.0. Biomass was washed three times with buffer to eliminate residual substrates. To establish anaerobic conditions, both the liquid phase and headspace were purged with argon. The vials were then incubated at 35 °C with agitation at 120 rpm until pressure stabilized. Substrates were injected aseptically through rubber septa as follows: 42 mg N L^{-1} of a mixture of $(NH_4)_2SO_4$ and $NaNO_2$ for SAA, and 100 mg N–NO_3^- L^{-1} plus 450 mg C L^{-1} (as acetate) for SDA. Nitrogen gas production was monitored by measuring pressure increases, and specific metabolic activities were calculated accordingly. Control vials without added substrates were used to account for endogenous respiration. All experiments were conducted in triplicate.

2.2.2. Physical characterization. The diameter of the AGS was measured using MonGran software, as proposed by Jara-Muñoz *et al.*[19] At least 370 samples were collected to determine the size distribution. The AGS surface was analyzed by SEM. Sample preparation involved washing, fixing, and drying following the methodology proposed by Guzmán-Fierro *et al.*[20]

2.2.3. Chemical characterization. The analysis of functional groups in the AGS was performed using Fourier transform infrared spectroscopy (FTIR).[21] Samples were dried at 105 °C for 15 h before analysis. The IR spectra were collected over the range of 400–4000 cm^{-1}. Cations (*e.g.*, copper, calcium, magnesium, iron, manganese, chromium, zinc, and lead) were identified and quantified *via* ion chromatography coupled with inductively coupled plasma-mass spectrometry (IC-ICP-MS) according to Peña-Farfal *et al.*[22]

2.2.4. Bacterial community characterization. Genomic DNA was extracted from AGS samples according to Murillo *et al.*[23] DNA was purified using the UltraClean DNA extraction Kit (MoBio, Carlsbad, USA), and its quality and concentration were assessed using a NanoDrop ND-1000 UV/Vis spectrophotometer (Peq-lab, Erlangen, Germany).[24] 16S rRNA (variable region 4) amplicons were sequenced on the Illumina HiSeq platform, producing 380 bp paired-end reads at Genoma Mayor (Universidad Mayor, Santiago, Chile). Preprocessing of sequencing data (quality checks and chimaera removal) was conducted using the DADA2 package. Taxonomic classification was performed with the SILVA v132 database using a native Bayesian classifier. Taxonomic composition was visualized using the Phyloseq R package and Krona software.

2.3. Reactor setup and operation for producing aerobic granular sludge

AGS was cultivated in a 2-liter SBR operated at 30 °C. The reactor was initially inoculated with mature AGS previously described by Guzmán-Fierro *et al.*[25] Unlike previous work, no pre-treatment or co-substrate addition was used in this study. Instead, the AGS was directly exposed to raw, undiluted landfill leachate collected from a landfill with 14 years of operation (Table 1). The initial sludge concentration was set at 0.5 g VSS L^{-1}. The inoculum consisted of compact, spherical aerobic granules (see Sections 3.3 and 3.4 for detailed characterization). A schematic representation of the reactor configuration and operational connections is provided in Fig. S1.

A customized SBR cycle structure was designed to enhance granule development and promote microbial selection pressure. This configuration was developed based on preliminary tests evaluating COD and nitrogen transformation rates under anaerobic and aerobic conditions. The final cycle consisted of 27 minutes of influent feeding, 6 h anaerobic reaction, 17.3 h of aerobic reaction, 3 minutes of settling, and 3 minutes of effluent withdrawal (total cycle time of 24 h; HRT = 18 days). The 6 h anaerobic phase ensured complete uptake of readily biodegradable COD and supported storage-driven denitrification. In comparison, the 17.3 h aerobic phase was adjusted to keep ammonia oxidation as the limiting step and to ensure that free ammonia concentrations (FA) at the start of aeration were high enough to inhibit NOB and favor AOB enrichment. This long aerobic phase is in line with cycle configurations reported for AGS systems designed to enrich nitrifying and denitrifying populations in high-strength nitrogenous wastewaters.[4] During the aerobic phase, aeration was continuously supplied, and dissolved oxygen (DO) was checked regularly and maintained at

Table 1 Average chemical characteristics of raw landfill leachate used as aerobic granular sludge (AGS) influent[a]

Parameter	Concentration (mg L^{-1})
Manganese	104.6 ± 6.5
Chromium	0.9 ± 0.0
Magnesium	518.0 ± 48.5
Calcium	1608.7 ± 86.6
Iron	252.3 ± 44.2
Zinc	2.9 ± 0.2
Copper	0.5 ± 0.0
Lead	0.2 ± 0.0
COD	20603.0 ± 6909.4
NH_4^+-N	1889.6 ± 32.2
NO_3^-N	187.2 ± 23.8
pH	8.8 ± 0.2

[a] Values represent the mean ± standard deviation.

saturation levels, averaging 7.1 ± 0.1 mg L^{-1}. A photograph of the SBR system used for AGS cultivation, along with an image of the granular biomass, is provided in Fig. S2.

The reactor operation was divided into a 50-days start-up phase and a 148-days stabilization phase (198 days in total). This phased strategy enabled AGS to adapt to undiluted landfill leachate conditions. Throughout the operational period, reactor performance was monitored by evaluating granule size distribution, biomass retention, and nutrient removal.

2.4. Desorption and mineralization of polyvalent cations

Desorption assays were performed *ex situ* using biomass withdrawn from the reactor and processed in separate flasks. Desorption and subsequent mineralization to obtain the cations assimilated by AGS during landfill leachate treatment were systematically evaluated. The desorption process was adapted from Wang *et al.*,[26] who demonstrated that NaCl induces metal release through ionic competition and displacement at binding sites within the EPS matrix. Moreover, similar NaCl concentrations have been shown to cause moderate osmotic stress while preserving nitrogen and phosphorus metabolic pathways.[27] AGS samples (2.5 g TS L^{-1}) were incubated in 0.1 M NaCl solution at 35 °C with constant agitation at 120 rpm for 4 hours in a shaking incubator (BJPX-2008, Biobase, China). The agitation speed was selected to replicate shear stress conditions comparable to those observed in reactor operations, as described by Jara-Muñoz *et al.*[19] Then, the supernatant was collected and analyzed for cation content.

For mineralization, the desorbed AGS granules were subjected to acid digestion. This process disrupted both cellular and EPS structures, replacing bound metal cations with protons (H^+), and promoting their release. This procedure was adapted from the method reported by Liu *et al.*[28] The granules were placed in test tubes containing concentrated nitric acid (65%) and heated at 105 °C for 15 minutes on a hot plate. After cooling, the digested samples were homogenized and analyzed for cation content.

2.5. Statistical analysis

All experiments were conducted in triplicate. Statistical analyses were performed using the Software GraphPad Prism v5.0 (GraphPad Software, USA). Results are expressed as mean ± standard deviation (SD). The differences between AGS with or without treatment (metal assimilation and metabolic activity) were evaluated using Student's *t*-test. The $p < 0.05$ was considered statistically significant.

3. Results and discussion

3.1. Designing the cycle structure for AGS reactor operating under SBR regime

The behaviour of COD and nitrogen species during the aerobic and anaerobic phases of the cycle is shown in Fig. 1. These profiles reflect the dynamic transformations that occur in the AGS reactor when exposed to raw, undiluted landfill leachate.

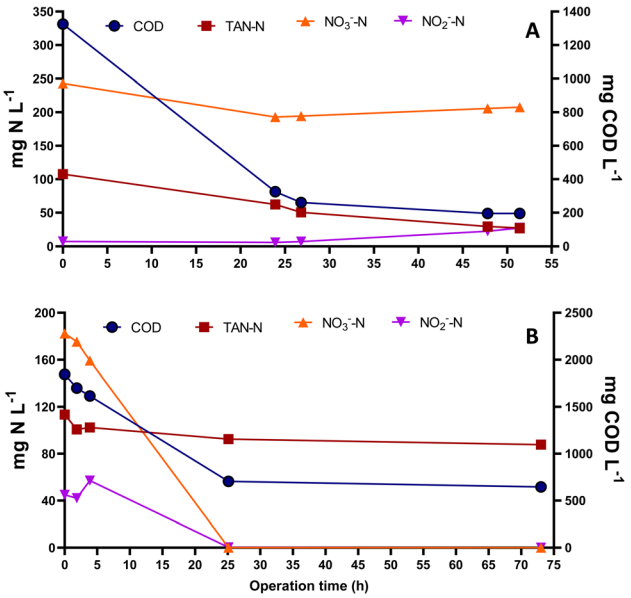

Fig. 1 Concentration profiles of COD and nitrogen species during cycle tests in the aerobic granular sludge (AGS) reactor using raw landfill leachate. (A) Aerobic phase. (B) Anaerobic phase. Reactor volume = 2.0 L and T = 30 °C. COD, chemical oxygen demand; TAN, total ammonia nitrogen.

3.1.1. Aerobic phase. During the 52-hours aerobic period, COD decreased from 1325 mg L^{-1} to 195 mg L^{-1}, corresponding to an overall removal of 85% (Fig. 1A). Most of this reduction occurred within the first 24 hours, when COD declined to 325 mg L^{-1} (75.5% removal), driven mainly by aerobic heterotrophic oxidation under fully oxygenated conditions (DO ≈ 7.1 mg L^{-1}).

Nitrogen species also showed active transformation. The concentration of TAN decreased from 108 to 62 mg N L^{-1} during the first 24 hours, while nitrate decreased from 243 to 193 mg N L^{-1}. Nitrite remained <10 mg N L^{-1} over most of the phase. These trends indicate simultaneous ammonium oxidation and aerobic denitrification facilitated by internal oxygen gradients within the granules, a behaviour previously reported in high-strength nitrogenous wastewaters treated under single-stage systems.[10]

Toward the end of the aerobic stage, nitrate and nitrite concentrations increased by 7.6% and 282%, respectively. This behaviour reflects the lower organic matter availability at later stages, which reduces oxygen competition and shifts the balance among nitrifying and heterotrophic populations. At this point, 85% of COD and 27% of total nitrogen had been removed.

3.1.2. Anaerobic phase. The anaerobic phase began after introducing a 5.5% exchange volume of landfill leachate, reaching an initial TAN concentration of 100 mg N L^{-1} in the reactor. Dissolved oxygen was depleted within 5 hours, establishing strict anaerobic conditions (Fig. 1B). Over the 73-hours anaerobic period, COD decreased by 65%, with the most pronounced decline (62%) occurring in the first 25 hours at a rate of 44 mg L^{-1} h^{-1}. This rapid decrease was associated first with residual aerobic oxidation (0–5 h) and subsequently with

denitrification using nitrate and nitrite. Both nitrate and nitrite were consumed entirely after 25 hours.

TAN remained relatively stable after 27 hours, with a slight decrease observed toward the end of the anaerobic period, indicating limited anaerobic ammonium transformations under the imposed conditions.

3.1.3. Nitrogen transformation dynamics. The nitrogen conversion patterns observed across the cycle reflect the competition among AOB, NOB, and aerobic heterotrophic bacteria (AHB). Competition for oxygen among these groups directly affects their apparent half-saturation coefficients, as noted in previous studies.[29]

AHB possess a higher oxygen affinity (AHB > AOB > NOB), allowing them to dominate oxygen uptake at elevated C/N ratios.[15,30,31] Their rapid consumption of organic substrates generates localized oxygen-limited zones that restrict NOB growth while maintaining partial nitrification.

The accumulation of nitrite toward the end of the aerobic phase is consistent with these dynamics: reduced organic matter alleviates oxygen limitation, enabling AOB activity. At the same time, free ammonia continues to suppress NOB.

3.1.4. Implications for cycle design. The operational cycle applied in this study was defined based on measured transformation rates. The 6-hours anaerobic phase supported efficient denitrification and COD uptake by storage-driven heterotrophs. The subsequent 17.3-hours aerobic phase was designed to maintain ammonia oxidation as the rate-limiting step.

The target TAN concentration of 30 mg N L^{-1} at the end of aeration corresponds to approximately 10 mg NH_3–N L^{-1} of free ammonia[17] —sufficient to inhibit NOB while preserving AOB activity, as reported by Anthonisen *et al.*[32] Sedimentation conditions were tuned to selectively retain granules exhibiting settling velocities greater than 3 m h^{-1}, thereby promoting robust granulation.[31] This selection pressure was further reinforced through short settling times (3 min) and the use of a bubble column reactor (BCR), in which gas-induced shear stress maintains granule stability even under long hydraulic retention times. This behaviour is consistent with the findings of Jara-Muñoz *et al.*,[19] who demonstrated improved sedimentation and microbial activity in gas-mixed systems.

Granules larger than 1.6 mm were consistently retained, confirming stable granulation under high-strength leachate conditions, as previously reported for similar operational strategies.[31] Aerobic conditions accounted for 73% of the cycle, exceeding the minimum aeration time required for sustained aerobic granulation.[33]

Overall, the cycle performance confirms that AGS can maintain carbon and nitrogen removal under undiluted landfill leachate conditions while preserving the selective pressures needed for robust granulation and partial nitrification.

3.2. Stabilizing organic and nitrogen removal in AGS reactor treating raw landfill leachate

The operation of the AGS reactor was divided into two distinct phases: a 50-days start-up period and a 148-days stabilization phase (198 days in total) (Fig. 2). During the start-up phase, the influent COD remained stable, with concentrations between 16 740 and 18 470 mg L^{-1} (Fig. 2A). COD values in effluent were consistently low, generally below 1500 mg L^{-1}, indicating that the system achieved substantial organic matter removal even during early granulation.

During the first 15 days of the start-up stage, the reactor was operated in batch mode to facilitate sludge acclimation and optimize the cycle configuration. A key challenge during this stage was the accumulation of FA on days 20 and 36, with concentrations peaking at 86 mg NH_3–N L^{-1} and 37 mg NH_3–N L^{-1}, respectively. Elevated FA levels can have toxic effects on microbial communities, impairing the nitrification. To mitigate, two aerobic batch treatments were implemented to promote the development of the nitrifying layer within the AGS. By day 50, the reactor was successfully transitioned to an SBR regime, which was maintained for the remainder of the experiment. Anthonisen *et al.*[32] reported that *Nitrosomonas* and *Nitrobacter* are inhibited at FA concentrations of 10–150 mg L^{-1} and 0.1–1.0 mg L^{-1}, respectively. Despite FA levels near 86 mg L^{-1}—within the inhibitory range—ammonia oxidation was sustained. This suggests microbial acclimation and a protective role of EPS, which may buffer or reduce FA

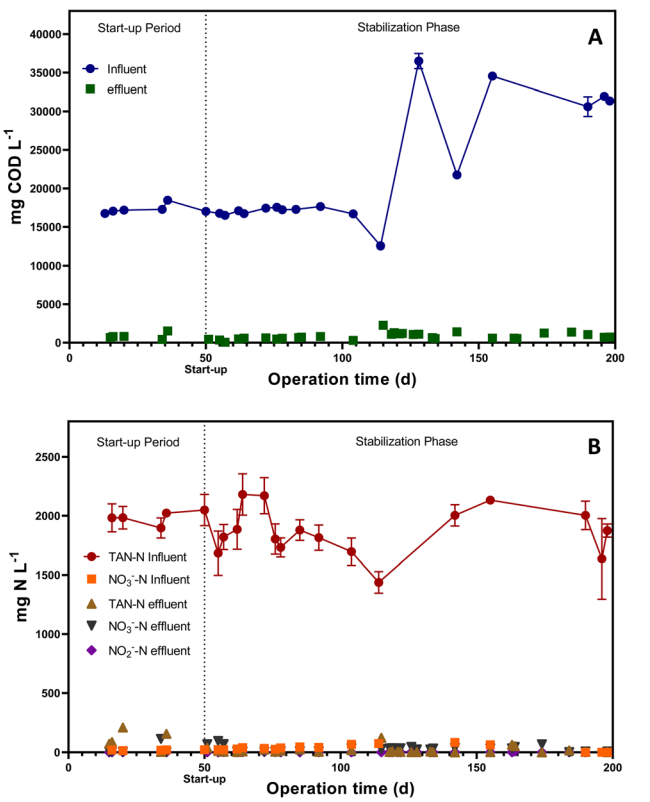

Fig. 2 Long-term performance of aerobic granular sludge (AGS) treating undiluted landfill leachate in an SBR. (A) Influent and effluent COD concentrations. (B) Influent and effluent nitrogen species: TAN, NO_3^-–N, and NO_2^-–N. Reactor volume = 2.0 L, HRT = 18 days and T = 30 °C. COD, chemical oxygen demand; TAN, total ammonia nitrogen. Note: each point represents the average of three replicates (n = 3). Error bars are present but may not be visible due to minimal variation and overlap with the data symbols.

diffusion. This observation underscores the robustness of the AGS and its potential to treat N-rich leachates without dilution.

When the system transitioned to stabilization phase, the COD influent increased noticeably, with peaks reaching over 34 000 mg L^{-1}, doubling typical concentration on days 128 and 155 (Fig. 2A). Despite these fluctuations, effluent COD concentrations remained low throughout the entire period (below 1500 mg L^{-1}), demonstrating the resilience and stability of the AGS system under elevated and variable organic loading. This performance suggests effective metabolic adaptability of the microbial community. Overall, COD removal remained above 94%, highlighting the robustness of the system for treating undiluted landfill leachate. The increase in biomass concentration to 5.9 g VSS L^{-1} also suggests effective granule retention and selective biomass accumulation. This gradual biomass build-up was driven by a moderate organic loading rate (OLR) (1.14 kg COD m^{-3} d^{-1}). This strategy aimed to accommodate the complex matrix and potential inhibitory effects of raw landfill leachate. The development of dense, well-structured granules may have contributed to shock absorption and sustained metabolic activity. These findings support the potential scalability of AGS for treating complex, non-diluted landfill leachates, while minimizing energy input and co-substrate demand. Nitrogen removal performance followed a similarly stable trend (Fig. 2B). Performance was evaluated during the start-up (0–50 days) and stabilization (51–198 days) phases of reactor operation. During the entire period, the influent TAN remained high, fluctuating between 1436 and 2181 mg N L^{-1}, while nitrate (NO_3^-–N) levels in the influent were generally below 90 mg N L^{-1}. Despite the elevated nitrogen loads in TAN, effluent TAN was effectively reduced to values below 45 mg N L^{-1} during the stabilization phase, with most measurements falling under 30 mg N L^{-1}, indicating robust ammonium oxidation. Similarly, effluent concentrations of nitrate and nitrite remained consistently low, typically under 60 mg N L^{-1}, suggesting that denitrification was active and efficient under the reactor's operational conditions. Notably, even during periods of increased influent TAN, particularly between days 64, 72, and 155, the system maintained stable nitrogen removal, with no relevant accumulation of nitrate or nitrite in the effluent. These results reflect the establishment of a functionally stratified microbial community within the granules, capable of supporting undiluted leachate conditions. Most studies on landfill leachate treatment using AGS rely on dilution strategies to manage high organic and nitrogen loads. For example, Bueno *et al.*[10] achieved COD and nitrogen removal efficiencies of 88% and 99%, respectively, by treating 20% diluted landfill leachate under an OLR of 2.56 kg COD m^{-3} d^{-1} and a nitrogen loading rate (NLR) of 0.51 kg N m^{-3} d^{-1}. Similarly, Seid-Mohammadi *et al.*[34] reported COD and TAN removal efficiencies of 39–80% and 45–74%, respectively, using leachate diluted to 20–50%, with OLRs of 18–76 g COD m^{-3} d^{-1} and NLRs of 1.1–2.4 g N m^{-3} d^{-1}.

In contrast, our study operated under more challenging conditions, using raw (undiluted) landfill leachate as the sole feed. During the stabilization phase, the reactor consistently maintained high COD and nitrogen removal efficiencies of 94% and 97%, respectively, even under an OLR of 1.14 kg COD m^{-3} d^{-1} and NLR of 0.12 kg N m^{-3} d^{-1}. These results confirm that granule formation and functional microbial stratification can be achieved without dilution. This is likely due to the extended SBR cycle and controlled oxygen strategy applied during start-up. These findings underscore the potential of AGS reactors for treating raw landfill leachate. The system's resilience and efficiency provide key insights for scaling up AGS technology, contributing to more sustainable leachate management. Our results are consistent with other studies using AGS. For example, Seid-Mohammadi *et al.*[34] reported over 98% COD removal and successful granule formation in a GSBR operated under similar DO and pH conditions. The comparable granule structure and treatment efficiency observed in our system further support the viability of AGS for treating complex, high-strength effluents without dilution or co-substrate addition.

3.3. Polyvalent cations in aerobic granular sludge: biosorption and bioaccumulation

The biosorption and bioaccumulation of polyvalent cations in AGS were evaluated using a two-step sequential extraction method. First, cation desorption with NaCl was performed to quantify the biosorbed fraction; second, acid digestion was used to determine the bioaccumulated fraction. This approach allows differentiation between cations weakly bound to the surface and those retained within the microbial or structural matrix of the granules.

The characterization of the landfill leachate and the assimilation of cations by AGS are summarized in Tables 1, 2 and S2. A total of 600.47 μmol g^{-1} TS of cations were assimilated, of which 53% corresponded to biosorption and 47% to bioaccumulation. Magnesium predominated in the biosorbed fraction, with 179.6 μmol g^{-1} TS (56.74%), followed by calcium with 116.4 μmol g^{-1} TS (36.77%) and iron with 14.26 μmol g^{-1} TS (4.50%). In contrast, in the bioaccumulated fraction, the dominant cation was calcium, with 86.15% (244.6 μmol g^{-1} TS), followed by magnesium with 5.20% (14.77 μmol g^{-1} TS) and iron with 4.97% (14.11 μmol g^{-1} TS). Considering total cation assimilation (biosorption + bioaccumulation), calcium was the most abundant (60.12%, 361 μmol g^{-1} TS), followed by magnesium (32.37%, 194.37 μmol g^{-1} TS), iron (4.72%, 28.37 μmol g^{-1} TS), and manganese (1.85%, 11.12 μmol g^{-1} TS). This distribution accurately reflects the cationic composition of the landfill leachate (Table 1), where calcium was also dominant (59.08%), followed by magnesium (31.37%), iron (6.65%), and manganese (2.8%) (Table 1). These results suggest a selective assimilation mechanism by AGS biomass aligned with influent composition.

3.3.1. Cation-specific retention and functional roles. Among all cations, calcium showed the highest degree of bioaccumulation (244.6 μmol g^{-1} TS), representing 86.15% of the total bioaccumulated fraction. This behavior is consistent with the established role of calcium as a structural component within the AGS, mainly through its interaction with the EPS, which improves the cohesion and integrity of the granules.[35] However, the high calcium content may also result from

intragranular precipitation, especially under alkaline conditions. The observed accumulation was detectable only after acid digestion, suggesting the formation of precipitated species, such as calcium carbonate. The alkaline pH of the reactor (~8.8), together with the generation of carbonate during denitrification, probably favored this process.[36] Similar findings have been reported in AGS systems, where elevated calcium concentrations (>90 mg g^{-1} SS) reduced bioactivity due to clogging of internal structures.[37]

Beyond structural roles, calcium also participates in intracellular signaling. Under basal conditions, intracellular calcium concentrations range between 0.09 and 0.3 μM, but can increase up to 5.4 μM through protein-mediated binding in response to environmental stimuli.[38] Calcium, therefore, plays a dual role in AGS: as a structural stabilizer through EPS interactions and as a regulatory ion involved in microbial function. In addition, calcium assimilation may be influenced by granule size, as larger granules tend to have higher EPS content and longer diffusion pathways, which improves metal retention.[39]

In contrast, magnesium showed the highest biosorption among all cations (179.6 μmol g^{-1} TS), accounting for 92.4% of its total assimilation, with only 7.6% through bioaccumulation. This behavior, which is opposite to that of calcium, highlights the existence of specific retention mechanisms for each cation, probably governed by factors such as hydration radius, coordination chemistry, and affinity for EPS functional groups.[35]

3.3.2. Iron and manganese retention behavior. Iron showed a balanced distribution between biosorption (14.26 μmol g^{-1} TS) and bioaccumulation (14.11 μmol g^{-1} TS), with no statistically significant difference ($p = 0.8272$). This balance suggests complexation mechanisms involving both EPS binding and intracellular incorporation. Iron plays a fundamental role in AGS granulation, as it contributes to bio-coagulation by facilitating the formation of dense aggregates with a high specific gravity.[35] Its retention in AGS may occur through complex chemical structures, such as iron phosphate or iron sulfide species, rather than through simple electrostatic interactions. In addition, Fe^{2+} biosorption capacities up to 232 mg g^{-1} have been reported at acidic pH (2.4–3.4), suggesting that pH-dependent speciation influences assimilation efficiency.[40]

Manganese showed a strong tendency for bioaccumulation (87.6%, 9.74 μmol g^{-1} TS), with only 12% retained by biosorption. This suggests that manganese is preferentially internalized or forms stable complexes within the microbial matrix. Its bioaccumulation ratio was 69% higher than that of calcium, highlighting its distinctive retention behavior, which may be related to its role in enzymatic systems and redox processes.

3.3.3. Trace metals and recovery efficiency. Although trace cations such as copper, chromium, zinc, and lead were assimilated at lower concentrations, they showed high recovery efficiencies (>77%) *via* biosorption (Table 2). Copper showed the highest recovery efficiency, at 93.6%, followed by lead (92.9%), chromium (89.6%), and zinc (77.3%). This behavior indicates strong surface affinity and suggests that these metals are readily recoverable *via* mild desorption processes.

The high biosorption of copper implies promising potential for the reuse of AGS as a biosorbent in metal recovery applications. In contrast, calcium showed the lower recovery efficiency (32.2%), reinforcing its strong binding within the AGS matrix. These differences highlight the importance of understanding the specific cation retention mechanisms when designing strategies for selective recovery and valorization of metals in wastewater treatment. In the context of a closed-loop recovery scheme, the NaCl desorption step used here yields a metal-rich eluate containing trace metals such as Cu, Pb, Cr, and Zn at higher concentrations than in the original leachate. This eluate can serve as a suitable feed stream for downstream recovery operations—such as selective precipitation, crystallization, or electrochemical extraction—to produce reusable metal concentrates. At the same time, the bulk liquid phase can be recycled. Although these downstream concentration and purification stages were not implemented in the present work, our results demonstrate that AGS can (i) capture metals directly from undiluted landfill leachate and (ii) release them under mild conditions into a separate liquid stream without compromising granule integrity. This two-step sequence constitutes the core of a regenerative biosorption cycle and provides the necessary input for future development of fully closed-loop metal recovery systems.

Table 2 Quantification of polyvalent cation assimilation by aerobic granular sludge (AGS) through biosorption (NaCl desorption) and bioaccumulation (acid digestion)[a]

Cation	Biosorption (μmol g^{-1} TS)	Bioaccumulation (μmol g^{-1} TS)	*P*-value	Total cation assimilation (μmol g^{-1} TS)	Desorption recovery efficiency (%)
Manganese	1.38 ± 0.76	9.74 ± 0.44	<0.0001	11.12	12.4
Chromium	1.46 ± 0.08	0.17 ± 0.01	<0.0001	1.63	89.6
Magnesium	179.60 ± 3.99	14.77 ± 0.47	<0.0002	194.37	92.4
Calcium	116.40 ± 16.76	244.60 ± 7.36	0.0003	361.00	32.2
Iron	14.26 ± 0.99	14.11 ± 1.13	0.8272	28.37	50.3
Zinc	1.29 ± 0.11	0.38 ± 0.09	0.0004	1.67	77.3
Copper	2.03 ± 0.32	0.14 ± 0.05	0.0004	2.17	93.6
Lead	0.13 ± 0.00	0.01 ± 0.00	<0.0001	0.14	92.9

[a] Values represent the mean ± standard deviation of three replicates ($n = 3$). Statistical significance was assessed using the student's *t*-test, with a threshold of $p < 0.05$. TS, total solids.

To further enhance recovery yields, particularly for less desorbable cations such as calcium and manganese, future work should explore optimization of desorption parameters, including NaCl concentration, contact time, and pH adjustment. However, any such modifications must preserve granule structure and microbial functionality to ensure that improved recovery performance does not undermine biological treatment efficiency.

The desorption trends observed here are consistent with previous studies, which indicate that chloride ions enhance metal release from solid matrices by weakening coordination interactions. Long *et al.*[41] demonstrated that Cl^- disrupts metal–surface binding, improving leaching efficiency. These findings support the selection of NaCl as a mild and effective desorption agent, particularly in EPS-rich systems such as AGS.[42]

3.4. Effect of the desorption process on aerobic granular sludge

The morphological properties, metabolic activities, and bacterial community composition of AGS were evaluated before and after mild desorption treatment with 0.1 M NaCl.

3.4.1. Morphological effects. No statistically significant change in granule size distribution was observed before and after desorption ($p = 0.059$) (Fig. S3). The mean diameters were 1.63 mm ± 0.75 and 1.73 mm ± 0.62 in the AGS before and after treatment, respectively. A positive correlation between the diameter and the sedimentation properties of the AGS has been previously reported.[15] Therefore, NaCl treatment did not affect the retention capacity in granular reactors, which are known to be controlled by the sedimentation rate of the AGS. The SEM images of aerobic granules before and after the desorption treatment show no evident changes that could affect their function (Fig. S4). In both conditions, a filamentous matrix was observed surrounding the microbial aggregates, suggesting a key structural role. Bacterial morphotypes resembling bacilli and cocci are distinguishable, with no clear evidence of predominance. The 2 μm images reveal internal cavities, presumably associated with granule pores. According to Chen *et al.*[42] and Hou *et al.*,[43] these cavities serve as channels for substrate transport from the surrounding liquid to the interior of the granule. Additionally, they propose that filamentous structures contribute to mechanical stability and promote the development of AGS.

3.4.2. Chemical characterization. FTIR analysis (Fig. 3) was performed to compare the molecular structures and functional groups of AGS before and after desorption. The spectra revealed consistent peak positions across both samples, indicating preserved chemical functionality, but with notable differences in absorption intensities at key regions associated with EPS-metal interactions. At 3290 cm^{-1}, the spectrum after desorption exhibited approximately 30% higher absorption compared to the sample before desorption. This region corresponds to O–H and N–H stretching vibrations, commonly found in water, alcohols, and proteins.[44] Gao *et al.*[45] reported similar findings in biosorption studies, attributing this peak to hydrogen-bonded hydroxyl and amine groups. The increased absorption is likely due to sodium interaction following the NaCl-induced

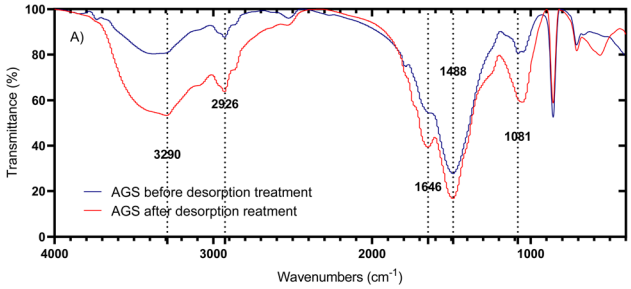

Fig. 3 FTIR characterization of aerobic granular sludge (AGS) before and after desorption using NaCl (0.1 M).

desorption. The band at 2926 cm^{-1}, related to CH_2 and CH_3 stretching in aliphatic chains,[44] showed a double peak in both spectra. A slightly more pronounced signal after desorption suggests subtle rearrangements within aliphatic structures, possibly due to ionic interactions with the EPS matrix.[45] At 1646 cm^{-1}, which represents C=O and C–N stretching of amide I, a 16% increase in absorption was observed after desorption. This band is characteristic of peptide bonds in proteins, indicating their involvement in metal retention.[45] Zhou *et al.*[46] similarly associated this region with amide I and II groups in AGS. The peak at 1488 cm^{-1} showed the most notable difference, with transmittance decreasing from 27.8% before to 16.9% after desorption, indicating stronger absorption.

This band corresponds to asymmetric C–O stretching in polysaccharides and proteins.[44] The change supports previous findings that carboxyl groups in EPS play a central role in cation binding.[28] At 1081 cm^{-1}, associated with O–H stretching in polysaccharides,[45,46] the spectrum after desorption showed increased intensity, suggesting that hydroxyl groups also participated in the reversible coordination with metal ions. Below 1000 cm^{-1}, bands linked to phosphate group vibrations[47] mainly remained unchanged, indicating minimal involvement in the desorption process.

Taken together, the FTIR analysis confirmed the involvement of three major functional groups in metal binding: hydroxyl (O–H), amide (C=O and C–N), and polysaccharidic (C–O). Although several bands showed intensity changes, no new peaks emerged, and the spectral pattern remained stable. This indicates that desorption successfully removed the metal without compromising the AGS's structural integrity or its functional groups. These findings are consistent with Liu *et al.*,[11] who reported the persistence of EPS functionality after exposure to heavy metals. The increased absorption intensity of the amide and hydroxyl regions after desorption confirms their key roles in metal retention and release.[48,49] The preservation of active sites post-desorption further supports the reuse potential of AGS in multiple biosorption cycles.[50]

3.4.3. Metabolism effects. Metabolic characterization of the specific activities of AGS before and after desorption was conducted (Table 3). Aerobic metabolism varied across the processes evaluated. There was no evidence of SNOA in the analyzed samples; this suggests that competition for oxygen by AOB and for nitrite by anammox or denitrifiers was avoided.[17]

Table 3 Metabolic activity of aerobic granular sludge (AGS) before and after NaCl (0.1 M) desorption treatment[a]

Parameter	AGS without treatment	AGS with treatment	*p*-Value
SAOA (g N–NH_4^+ g^{-1} VSS d^{-1})	0.011 ± 0.0004	0.003 ± 0.0005	<0.0001
SNOA (g N–NO_2^- g^{-1} VSS d^{-1})	0 ± 0	0 ± 0	—
SHA (g O_2 g^{-1} VSS d^{-1})	0.452 ± 0.0075	1.101 ± 0.3074	0.0217
SAA (g N_2 g^{-1} VSS d^{-1})	0.314 ± 0.08	0.286 ± 0.046	0.7321
SDA (g N_2 g^{-1} VSS d^{-1})	0.958 ± 0.057	0.523 ± 0.071	0.0012

[a] Values represent the mean ± standard deviation. Statistical significance was assessed using the student's *t*-test, with a threshold of $p < 0.05$. SHA, specific heterotrophic activity; SAOA, specific ammonium-oxidizing activity; SNOA, specific nitrite-oxidizing activity; SAA, specific anammox activity; SDA, specific denitrification activity.

SAA showed no significant difference with NaCl treatment (*p*-value = 0.7321). Recently, Xu *et al.*[51] described a salt tolerance mechanism in partial denitrification and anammox processes. They reported that anammox activity was maintained even at 0.17 M of NaCl, achieving 81% of nitrogen removal. On the other hand, in our work, the SAOA decreased 3.7-fold with the NaCl treatment, and the SDA decreased 1.8-fold. Similar findings were reported for nitrification activity by Zhao *et al.*,[52] who demonstrated that NaCl exposure in an SBR reduced ammonia removal from 95% at 0.3 M to 25% at 0.5 M.[52] In addition, Wang *et al.*[53] evaluated AGS at salinity levels ranging from 0% to 8%, observing 9.2 and 4.7-fold decreases in SAOA and SDA, respectively. Thus, as in our work, Wang *et al.*[53] demonstrated that denitrifying activity is more tolerant of increased salinity compared to nitrification. Meanwhile, in our work, SHA increased 2.4-fold with NaCl treatment. A similar result was also reported by Wang *et al.*,[53] who found that SHA increased 1.4-fold at 3% salinity. NaCl desorption primarily affects nitrogen removal pathways in AGS. However, it enhances organic heterotrophic activity.

3.4.4. Bacterial community analysis. To better understand the biological basis for the observed metabolic changes, the composition of the AGS microbial community was analyzed before (BD) and after (AD) cation desorption treatment. Metagenomic analysis of the 16S rRNA gene revealed 21 distinct bacterial phyla in both conditions.

In the BD sample, the dominant phyla (relative abundance ≥1%) were Proteobacteria (57.1%), Firmicutes (35.4%), Actinobacteria (2.2%), and Bacteroidetes (2.1%) (Fig. 4). Within Proteobacteria, the most abundant classes were Betaproteobacteria (20.7%), Alphaproteobacteria (18.6%), Gammaproteobacteria (16.4%), and Deltaproteobacteria (1.3%). In the AD sample, Proteobacteria increased to 85.4%, while Firmicutes decreased to 10.1%. Actinobacteria and Bacteroidetes also decreased slightly to 1.2% and 1.4%, respectively. Betaproteobacteria dominated AD (74.0%), followed by Alphaproteobacteria and Gammaproteobacteria (both 5.6%). This shift suggests that the desorption treatment temporarily altered nutrient availability, favoring fast-growing heterotrophic taxa adapted to increased carbon accessibility.

In BD, sequences affiliated with Alphaproteobacteria were mainly classified as Rhizobiales (41.2%) and Rhodospirillales (4.2%), whereas in AD, Rhodobacterales (3.6%) emerged as the dominant order. The genus *Paracoccus* increased in AD (8.2%), consistent with literature reports describing *Paracoccus* as a metabolically versatile genus capable of aerobic growth on multicarbon substrates and facultative nitrate respiration under anoxic conditions.[54]

Betaproteobacteria was the dominant class in both BD and AD. In BD, major orders included Rhodocyclales (62.2%) and Nitrosomonadales (1.2%), with genera such as *Thauera* (15.5%)—a well-known denitrifier[55]—and *Nitrosomonas* (1.2%), an AOB commonly found in nitrifying systems.[56]

In contrast, the AD sample was mainly composed of Burkholderiales (37.9%), which includes heterotrophic genera such as *Burkholderia*, known for their biodegradation capacity and redox versatility.[57] It should be noted that *Nitrosomonas* was not detected in AD, suggesting that nitrification activity may have been affected after desorption.

Other orders detected exclusively in AD were Enterobacteriales and Pseudomonadales, each with a relative abundance ≥1% within the Gammaproteobacteria class. These groups include facultative heterotrophs capable of thriving under fluctuating redox and salinity conditions, typical of landfill leachate environments.[58,59]

The phyla Actinobacteria and Bacteroidetes, although present in relatively low abundance (<2.3%), are functionally important in organic matter turnover and the nitrogen cycle.

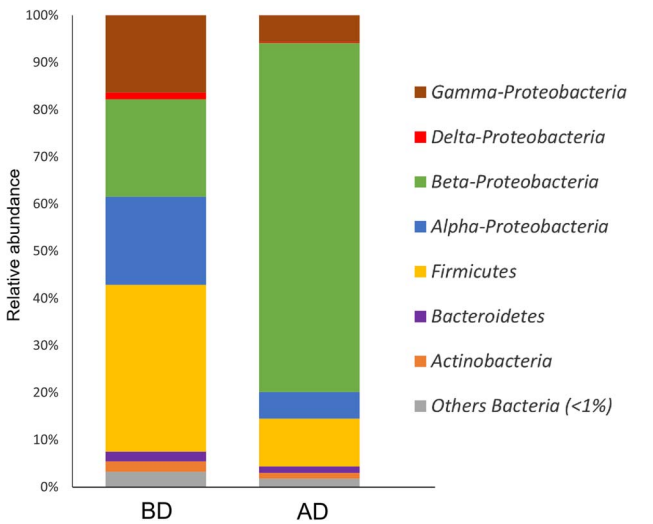

Fig. 4 Relative abundance of dominant taxonomic groups (abundance ≥1%) (percentage) assigned to bacterial phylogenetic groups collected from aerobic granular sludge (AGS) before (BD) and after (AD) desorption.

The genera *Sphingobacterium* and *Flavobacterium* have been involved in denitrification and the degradation of organic compounds,[62] however, they were not dominant under either condition in this study.

The loss of *Nitrosomonas* is in line with the pronounced decrease in SAOA observed in the metabolic assays (Table 3), indicating a loss of autotrophic ammonium-oxidizing capacity. Conversely, the increased relative abundance of *Paracoccus*, *Thauera*, and other facultative heterotrophs within Burkholderiales and Enterobacteriales is consistent with the marked increase in SHA and the decrease in SDA after NaCl treatment, reflecting a shift towards communities that are more active in heterotrophic COD removal but less efficient in nitrification and coupled denitrification.[54–57] The absence of detectable SNOA is consistent with the very low relative abundance of typical nitrite-oxidizing bacteria such as *Nitrospira* and *Nitrobacter* in the community profile. Overall, these taxonomic changes corroborate the functional trends revealed by the metabolic activity measurements. Although specific functional activities were not resolved at the strain level, these taxonomic assignments are consistent with the known roles of these genera in C and N cycling in wastewater systems and provide insight into how the complex microbial community supports the overall reactor performance.

Cation desorption was performed using 0.1 M NaCl at 35 °C for 4 hours, based on protocols that minimize disruption of the granules and allow for efficient release of the metals.[26] According to Yang *et al.*,[27] moderate salinity (~0.1 M) preserves the complexity of the microbial network and the abundance of functional genes, especially for the nitrogen and phosphorus cycles. Our findings support that this level of salinity induces moderate osmotic stress, leading to selective microbial changes without compromising the overall integrity of the AGS.

Although desorption temporarily altered the microbial composition and reduced nitrification, heterotrophic function and granule structure were preserved, allowing for sustained COD removal. Chu *et al.* [60] reported similar patterns and demonstrated that landfill microbial communities metabolically adapt to anaerobic phases depending on available electron acceptors (*e.g.*, nitrate, sulfate, Fe^{3+}). These results support the viability of a dual-function approach, in which part of the AGS can be periodically regenerated for metal recovery, while the rest maintains treatment performance. Furthermore, AGS subjected to NaCl desorption remains structurally intact and functionally active, allowing its reuse in subsequent biosorption cycles, thereby reducing biomass waste and operating costs. However, the long-term consequences of repeated desorption cycles are still unknown. Future studies should evaluate multi-cycle regeneration at the laboratory and pilot scale to determine AGS durability and microbial resilience. This reuse strategy supports AGS-based circular bioengineering by positioning landfill leachate as a source of recoverable resources rather than just a contaminant stream. In practical terms, periodic desorption of a fraction of the biomass would allow metals to be stripped into a concentrated side-stream. At the same time, the remaining AGS maintains treatment performance in the main reactor. Over successive sorption–desorption cycles, this configuration would support continuous removal of contaminants from landfill leachate and progressive accumulation of target metals in the eluate, thereby operationalising a regenerative, closed-loop metal recovery concept.

4. Conclusions

This study demonstrates that aerobic granular sludge is a resilient and multifunctional system. It effectively treats raw, undiluted landfill leachate while enabling resource recovery. The system achieved high removal efficiencies of COD and total nitrogen (94% and 97%, respectively), even under elevated organic and nitrogen loads, without dilution or co-substrate addition. These results highlight its robustness and scalability for real-world applications. Beyond pollutant removal, this work introduces a simple method to determine cation retention mechanisms. Biosorption and bioaccumulation contributed almost equally (53% and 47%, respectively), with calcium and magnesium as the dominant species. Using 0.1 M NaCl, we applied a mild desorption strategy that partially recovered biosorbed metals. FTIR, SEM, and metabolic assays confirmed that granule structure and heterotrophic activity were preserved. However, nitrification and denitrification activities were temporarily reduced, underscoring the need to balance recovery with treatment performance.

In the context of metal recovery, this work demonstrates the two core steps of a regenerative cycle: AGS captures metals from undiluted leachate and subsequently releases them into a metal-rich eluate under mild conditions. This eluate provides the necessary feed stream for downstream concentration or purification processes, offering a practical basis for future closed-loop recovery schemes.

Metagenomic analysis further revealed microbial shifts toward metabolically versatile genera following desorption. This indicates adaptive community responses under regenerative conditions. In particular, the loss of Nitrosomonas was consistent with the pronounced decrease in nitrifying activities. In contrast, the enrichment of heterotrophic and denitrifying genera, such as *Paracoccus*, *Thauera,* and members of Burkholderiales and Enterobacteriales, matched the increase in heterotrophic COD removal and the reduction in denitrification activity. These functional roles are inferred from 16S rRNA gene-based taxonomic profiles and literature reports, and they highlight how the microbial community underpins the process-level response to NaCl desorption. Together, these findings support a dual-process application of AGS: (1) continuous deployment for carbon and nutrient removal, and (2) periodic harvesting of granules for metal recovery *via* controlled desorption. This dual role reframes landfill leachate not just as a pollutant stream but as a recoverable resource, advancing circular economy strategies in wastewater management.

This study proposes a novel framework for treating complex effluents without chemical dilution while enabling resource recovery. Future research should explore operational strategies to sustain nitrification after desorption. Long-term experiments are needed to test whether AGS resilience persists under cyclic recovery. Such studies are essential to validate AGS-based regenerative systems in real-world applications.

Author contributions

V. Guzmán-Fierro: funding acquisition, conceptualization, supervision, data curation, project administration, writing – original draft. M. Quiroz: methodology, data curation, formal analysis. K. Moscoso: methodology, data curation, formal analysis. C. Arriagada: data curation, formal analysis, supervision. C. Espinoza: data curation, formal analysis. J. Mansilla: data curation, formal analysis. D. Contreras: resources, data curation. V. Campos: supervision, methodology, writing – original draft. J. J. Gallardo-Rodríguez: data curation, writing – original draft. G. Riveros: project administration, writing–review & editing. M. Roeckel: funding acquisition, supervision.

Conflicts of interest

There are no conflicts to declare.

Data availability

Some of the data generated during this study are included in this article. The rest datasets generated in the study are available from the corresponding author on reasonable request.

Supplementary information (SI): Fig. S1–S4 (AGS reactor scheme, experimental setup/biomass characteristics, granule diameter distribution with/without NaCl desorption, and SEM surface morphology) and Tables S1 and S2 (comparative overview of advanced leachate treatment technologies and detailed biosorption/bioaccumulation data for polyvalent cations, expressed in mg g^{-1} TS). See DOI: https://doi.org/10.1039/d5ra05817a.

Acknowledgements

This study was made possible by FONDEF (Chile) [grant number ID24I1045]; FONDECYT (Chile) [grant number 1200583]; FOVI (Chile) [grant number 240037]; CORFO INNOVA CHILE [grant number 17COTE-82999]; Agencia Nacional de Investigación y Desarrollo (ANID) [grant numbers PFCHA/DOCTORADO NACIONAL/2018–21180566, PFCHA/DOCTORADO NACIONAL/2018–21180541, PFCHA/DOCTORADO NACIONAL/2024–21241111]; and FONDEQUIP [grant number 180217].

Notes and references

1 J. P. Essien, D. I. Ikpe, E. D. Inam, A. O. Okon, G. A. Ebong and N. U. Benson, Occurrence and spatial distribution of heavy metals in landfill leachates and impacted freshwater ecosystem: an environmental and human health threat, *PLoS One*, 2022, **17**, e0263279.

2 L. Lindamulla, N. Nanayakkara, M. Othman, S. Jinadasa, G. Herath and V. Jegatheesan, Municipal solid waste landfill leachate characteristics and their treatment options in tropical countries, *Curr. Pollut. Rep.*, 2022, **8**, 273–287.

3 T. A. Kurniawan, P.-S. Yap and Z. Chen, Techniques for pollutant removal, nutrient recovery, and energy production from landfill leachates: a review, *Environ. Chem. Lett.*, 2025, **23**, 517–577.

4 Y. Wei, M. Ji, R. Li and F. Qin, Organic and nitrogen removal from landfill leachate in aerobic granular sludge sequencing batch reactors, *Waste Manage.*, 2012, **32**, 448–455.

5 S. Xie, Biosorption of heavy metal ions from contaminated wastewater: an eco-friendly approach, *Green Chem. Lett. Rev.*, 2024, **17**, DOI: 10.1080/17518253.2024.2357213.

6 T. Paul, J.-J. Yee and S. H. Park, Biochar-assisted aerobic granulation in enhanced biological treatment of landfill leachate with municipal wastewater for sustainable resource recovery: a biorefinery approach, *J. Environ. Chem. Eng.*, 2025, **13**, 115330.

7 L. Ruiz-Haddad, D. R. Shaw, M. Ali, M. Pronk, M. C. M. van Loosdrecht and P. E. Saikaly, Characterization of the core microbial community across different aggregate sizes in full-scale aerobic granular sludge plants and their relevance to wastewater treatment performance, *Water Res.*, 2025, **274**, 123036.

8 M. Pronk, M. K. de Kreuk, B. de Bruin, P. Kamminga, R. Kleerebezem and M. C. M. van Loosdrecht, Full scale performance of the aerobic granular sludge process for sewage treatment, *Water Res.*, 2015, **84**, 207–217.

9 V. Guzmán-Fierro, C. Arriagada, J. J. Gallardo, V. Campos and M. Roeckel, Challenges of aerobic granular sludge utilization: fast start-up strategies and cationic pollutant removal, *Heliyon*, 2023, **9**, DOI: 10.1016/j.heliyon.2023.e13503.

10 R. de F. Bueno, J. K. Faria, D. P. Uliana and V. S. Liduino, Simultaneous removal of organic matter and nitrogen compounds from landfill leachate by aerobic granular sludge, *Environ. Technol.*, 2021, **42**, 3756–3770.

11 C. Liu, Y. Shen, Y. Li, F. Huang, S. Wang and J. Li, Aerobic granular sludge for complex heavy metal-containing wastewater treatment: characterization, performance, and mechanisms analysis, *Front. Microbiol.*, 2024, **15**, DOI: 10.3389/fmicb.2024.1356386.

12 L. Britschgi, S. Wei, A. Proesl, E. Morgenroth and N. Derlon, The critical role of flocs in nitrification in full-scale aerobic granular sludge-based WWTP, *Water Res.*, 2025, **274**, 123021.

13 E. A. Giustinianovich, E. R. Aspé, J. E. Behar, V. L. Campos and M. D. Roeckel, Simultaneous removal of C and N from fish effluents in filter reactors: effect of recirculation ratio on the axial distribution of microbial communities, *J. Environ. Manage.*, 2015, **161**, 366–374.

14 O. Sánchez, E. Aspé, M. C. Martí and M. Roeckel, Rate of ammonia oxidation in a synthetic saline wastewater by a nitrifying mixed-culture, *J. Chem. Technol. Biotechnol.*, 2005, **80**, 1261–1267.

15 V. Guzmán-Fierro, J. Sanhueza, C. Arriagada, L. Pereira, V. Campos, J. J. Gallardo and M. Roeckel, The prediction of partial-nitrification-anammox performance in real industrial wastewater based on granular size, *J. Environ. Manage.*, 2021, **286**, 112255.

16 S. F. Yang, J. H. Tay and Y. Liu, Respirometric activities of heterotrophic and nitrifying populations in aerobic

granules developed at different substrate N/COD ratios, *Curr. Microbiol.*, 2004, **49**, 42–46.
17 C. Arriagada, V. Guzmán-Fierro, E. Giustinianovich, L. Alejo-Alvarez, J. Behar, L. Pereira, V. Campos, K. Fernández and M. Roeckel, NOB suppression and adaptation strategies in the partial nitrification–Anammox process for a poultry manure anaerobic digester, *Process Biochem.*, 2017, **58**, 258–265.
18 R. Varas, V. Guzmán-Fierro, E. Giustinianovich, J. Behar, K. Fernández and M. Roeckel, Startup and oxygen concentration effects in a continuous granular mixed flow autotrophic nitrogen removal reactor, *Bioresour. Technol.*, 2015, **190**, 345–351.
19 P. Jara-Muñoz, V. Guzmán-Fierro, C. Arriagada, V. Campos, J. L. Campos, J. J. Gallardo-Rodríguez, K. Fernández and M. Roeckel, Low oxygen start-up of partial nitrification-anammox process: mechanical or gas agitation?, *J. Chem. Technol. Biotechnol.*, 2019, **94**(2), 475–483.
20 V. G. Guzmán-Fierro, R. Moraga, C. G. León, V. L. Campos, C. Smith and M. A. Mondaca, Isolation and characterization of an aerobic bacterial consortium able to degrade roxarsone, *Int. J. Environ. Sci. Technol.*, 2015, **12**, 1353–1362.
21 B. C. Smith, *Fundamentals of Fourier Transform Infrared Spectroscopy*, CRC press, 2011.
22 C. Peña-Farfal, A. Moreda-Piñeiro, A. Bermejo-Barrera, P. Bermejo-Barrera, H. Pinochet-Cancino and I. de Gregori-Henríquez, Ultrasound Bath-Assisted Enzymatic Hydrolysis Procedures as Sample Pretreatment for the Multielement Determination in Mussels by Inductively Coupled Plasma Atomic Emission Spectrometry, *Anal. Chem.*, 2004, **76**, 3541–3547.
23 A. A. Murillo, S. RamÃrez-Flandes, E. F. DeLong and O. Ulloa, Enhanced metabolic versatility of planktonic sulfur-oxidizing γ-proteobacteria in an oxygen-deficient coastal ecosystem, *Front. Mar. Sci.*, 2014, **1**, 18.
24 C. Herrera, R. Moraga, B. Bustamante, C. Vilo, P. Aguayo, C. Valenzuela, C. T. Smith, J. Yáñez, V. Guzmán-Fierro, M. Roeckel and V. L. Campos, Characterization of arsenite-oxidizing bacteria isolated from arsenic-rich sediments, atacama desert, Chile, *Microorganisms*, 2021, **9**, 483.
25 V. Guzmán-Fierro, D. Salamanca, C. Arriagada, C. Espinoza, V. Campos, J. J. Gallardo and M. Roeckel, Efficient removal of nitrogen and organic matter strategy from landfill leachate under high seasonal substrate variations, *Environ. Technol. Innov.*, 2023, **32**, 103284.
26 L. Wang, C. Wan, D.-J. Lee, J.-H. Tay, X. F. Chen, X. Liu and Y. Zhang, Adsorption–desorption of strontium from waters using aerobic granules, *J. Taiwan Inst. Chem. Eng.*, 2013, **44**, 454–457.
27 C. Yang, Y. Chen, W. Sun, Q. Zhang, M. Diao and J. Sun, Extreme soil salinity reduces N and P metabolism and related microbial network complexity and community immigration rate, *Environ. Res.*, 2025, **264**, 120361.
28 W. Liu, J. Zhang, Y. Jin, X. Zhao and Z. Cai, Adsorption of Pb (II), Cd (II) and Zn (II) by extracellular polymeric substances extracted from aerobic granular sludge: efficiency of protein, *J. Environ. Chem. Eng.*, 2015, **3**, 1223–1232.
29 J. E. Baeten, M. C. M. van Loosdrecht and E. I. P. Volcke, Modelling aerobic granular sludge reactors through apparent half-saturation coefficients, *Water Res.*, 2018, **146**, 134–145.
30 W. Metcalf and C. Eddy, *Wastewater Engineering: Treatment and Resource Recovery*, 5th edn, 2014.
31 M. K. de Kreuk, M. Pronk and M. C. M. van Loosdrecht, Formation of aerobic granules and conversion processes in an aerobic granular sludge reactor at moderate and low temperatures, *Water Res.*, 2005, **39**, 4476–4484.
32 A. C. Anthonisen, R. C. Loehr, T. B. S. Prakasam and E. G. Srinath, Inhibition of nitrification by ammonia and nitrous acid, *J. - Water Pollut. Control Fed.*, 1976, 835–852.
33 S. L. de S. Rollemberg, T. J. T. Ferreira, P. I. M. Firmino and A. B. dos Santos, Impact of cycle type on aerobic granular sludge formation, stability, removal mechanisms and system performance, *J. Environ. Manage.*, 2020, **256**, 109970.
34 A. Seid-Mohammadi, G. Asgari, M. Rafiee, M. T. Samadi, F. Nouri, M. Pirsaheb and F. Asadi, The formation of aerobic granular sludge for the treatment of real landfill leachate using a granular sequencing batch reactor at a constant volume, *Environ. Qual. Manag.*, 2023, **32**, 135–146.
35 B. Kończak, J. Karcz and K. Miksch, Influence of calcium, magnesium, and iron ions on aerobic granulation, *Appl. Biochem. Biotechnol.*, 2014, **174**, 2910–2918.
36 J. R. Cunha, T. Tervahauta, R. D. van der Weijden, H. Temmink, L. Hernández Leal, G. Zeeman and C. J. N. Buisman, The effect of bioinduced increased pH on the enrichment of calcium phosphate in granules during anaerobic treatment of black water, *Environ. Sci. Technol.*, 2018, **52**, 13144–13154.
37 Y.-Q. Liu, G.-H. Lan and P. Zeng, Size-dependent calcium carbonate precipitation induced microbiologically in aerobic granules, *Chem. Eng. J.*, 2016, **285**, 341–348.
38 D. C. Domínguez, M. Guragain and M. Patrauchan, Calcium binding proteins and calcium signaling in prokaryotes, *Cell Calcium*, 2015, **57**, 151–165.
39 Z. Feng, H. Schmitt, M. C. M. van Loosdrecht and N. B. Sutton, Sludge size affects sorption of organic micropollutants in full-scale aerobic granular sludge systems, *Water Res.*, 2024, **267**, 122513.
40 K. H. Ahn and S. W. Hong, Characteristics of the adsorbed heavy metals onto aerobic granules: isotherms and distributions, *Desalin. Water Treat.*, 2015, **53**, 2388–2402.
41 Q. Long, H. Yan, H. Wu, S. Qiu, X. Zhou and T. Qiu, Influence mechanism of leaching agent anions on the leaching of aluminium impurities in ionic-type rare earth ores: a DFT simulation combined with experimental verification, *Sep. Purif. Technol.*, 2025, **354**, 128768.
42 X. Chen, L. Yuan, W. Lu, Y. Li, P. Liu and K. Nie, Cultivation of aerobic granular sludge in a conventional, continuous flow, completely mixed activated sludge system, *Front. Environ. Sci. Eng.*, 2015, **9**, 324–333.
43 Y. Hou, C. Gan, R. Chen, Y. Chen, S. Yuan and Y. Chen, Structural characteristics of aerobic granular sludge and

factors that influence its stability: a mini review, *MDPI*, 2021, **13**(19), 2726.

44 A. H. Kuptsov and G. N. Zhizhin, in *Handbook of Fourier Transform Raman and Infrared Spectra of Polymers*, ed. A. H. Kuptsov and G. N. Zhizhin, Elsevier, 1998, vol. 45, pp. 32–33.

45 J. Gao, Q. Zhang, K. Su, R. Chen and Y. Peng, Biosorption of Acid Yellow 17 from aqueous solution by non-living aerobic granular sludge, *J. Hazard. Mater.*, 2010, **174**, 215–225.

46 J. Zhou, F. Yang, F. Meng, P. An and D. Wang, Comparison of membrane fouling during short-term filtration of aerobic granular sludge and activated sludge, *J. Environ. Sci.*, 2007, **19**, 1281–1286.

47 Z. Wang, M. Gao, S. Wang, Y. Xin, D. Ma, Z. She, Z. Wang, Q. Chang and Y. Ren, Effect of hexavalent chromium on extracellular polymeric substances of granular sludge from an aerobic granular sequencing batch reactor, *Chem. Eng. J.*, 2014, **251**, 165–174.

48 C. Li, Y. Yu, A. Fang, D. Feng, M. Du, A. Tang, S. Chen and A. Li, Insight into biosorption of heavy metals by extracellular polymer substances and the improvement of the efficacy: a review, *Lett. Appl. Microbiol.*, 2022, **75**(5), 1064–1073.

49 Y. Xu, Y. Wu, S. Esquivel-Elizondo, J. Dolfing and B. E. Rittmann, Using microbial aggregates to entrap aqueous phosphorus, *Trends Microbiol.*, 2020, **38**(11), 1292–1303.

50 L. Huang, Y. Jin, D. Zhou, L. Liu, S. Huang, Y. Zhao and Y. Chen, A review of the role of extracellular polymeric substances (EPS) in wastewater treatment systems, *Int. J. Environ. Res. Public Health*, 2022, **19**(19), 12191.

51 A. Xu, D. Yu, Y. Qiu, G. Chen, Y. Tian and Y. Wang, A novel process of salt tolerance partial denitrification and anammox (ST-PDA) for treating saline wastewater, *Bioresour. Technol.*, 2022, **345**, 126472.

52 Y. Zhao, H.-D. Park, J.-H. Park, F. Zhang, C. Chen, X. Li, D. Zhao and F. Zhao, Effect of different salinity adaptation on the performance and microbial community in a sequencing batch reactor, *Bioresour. Technol.*, 2016, **216**, 808–816.

53 Z. Wang, M. Gao, Z. She, S. Wang, C. Jin, Y. Zhao, S. Yang and L. Guo, Effects of salinity on performance, extracellular polymeric substances and microbial community of an aerobic granular sequencing batch reactor, *Sep. Purif. Technol.*, 2015, **144**, 223–231.

54 D. P. Kelly, F. A. Rainey and A. P. Wood, in *The Prokaryotes*, Springer New York, New York, NY, 2006, pp. 232–249.

55 M. Atasoy, W. T. Scott Jr., K. van Gijn, J. J. Koehorst, H. Smidt and A. A. M. Langenhoff, Microbial dynamics and bioreactor performance are interlinked with organic matter removal from wastewater treatment plant effluent, *Bioresour. Technol.*, 2023, **372**, 128659.

56 E. G. Lauchnor, T. S. Radniecki and L. Semprini, Inhibition and gene expression of *Nitrosomonas europaea* biofilms exposed to phenol and toluene, *Biotechnol. Bioeng.*, 2011, **108**, 750–757.

57 V. C. Scoffone, G. Trespidi, G. Barbieri, S. Irudal, A. Israyilova and S. Buroni, Methodological tools to study species of the genus *Burkholderia*, *Appl. Microbiol. Biotechnol.*, 2021, **105**, 9019–9034.

58 L. Ding, B. Han and J. Zhou, Characterization of the facultative anaerobic Pseudomonas stutzeri strain HK13 to achieve efficient nitrate and nitrite removal, *Process Biochem.*, 2022, **118**, 236–242.

59 O. K. Aromolaran, O. Aromolaran, E. T. Faleye and H. Faerber, Environmental impacts of an unlined municipal solid waste landfill on groundwater and surface water quality in Ibadan, Nigeria, *Environ. Geochem. Health*, 2023, **45**(6), 3585–3616.

60 Y. Chu, X. Zhang, X. Tang, L. Jiang and R. He, Uncovering anaerobic oxidation of methane and active microorganisms in landfills by using stable isotope probing, *Environ. Res.*, 2025, **271**, 121139.